



저작자표시-비영리-변경금지 2.0 대한민국

이용자는 아래의 조건을 따르는 경우에 한하여 자유롭게

- 이 저작물을 복제, 배포, 전송, 전시, 공연 및 방송할 수 있습니다.

다음과 같은 조건을 따라야 합니다:



저작자표시. 귀하는 원저작자를 표시하여야 합니다.



비영리. 귀하는 이 저작물을 영리 목적으로 이용할 수 없습니다.



변경금지. 귀하는 이 저작물을 개작, 변형 또는 가공할 수 없습니다.

- 귀하는, 이 저작물의 재이용이나 배포의 경우, 이 저작물에 적용된 이용허락조건을 명확하게 나타내어야 합니다.
- 저작권자로부터 별도의 허가를 받으면 이러한 조건들은 적용되지 않습니다.

저작권법에 따른 이용자의 권리는 위의 내용에 의하여 영향을 받지 않습니다.

이것은 [이용허락규약\(Legal Code\)](#)을 이해하기 쉽게 요약한 것입니다.

[Disclaimer](#)

Thesis for the Degree of Master of Science

**On the freezing precipitation in Korea
and the basic schemes for its prediction**



by

Sang-Hoon Kwon

Department of Environmental Atmospheric Sciences

The Graduate school

Pukyong National University

August 2015



On the freezing precipitation in Korea and the basic schemes for its prediction

(한반도 어는 비와 그 예측을
위한 기본방안)

Advisor: Prof. Hi-Ryong Byun

by

Sang-Hoon Kwon

A thesis submitted in partial fulfillment of the requirements
for the degree of

Master of Science

in Department of Environmental Atmospheric Sciences,
The Graduate school, Pukyong National University

August 2015

On the freezing precipitation in Korea and the basic schemes for its
prediction

A dissertation
by
Sang-Hoon Kwon

Approved by:

(Chairman)

Jae-Jin Kim

(Member)

Byung-Hyuk Kwon

(Member)

Hi-Ryong Byun

August 21, 2015

CONTENTS

Contents	i
List of Figures	iv
List of Tables	v
Abstract	2
1. Introduction	6
2. Data	6
2.1 On the observation and records	8
2.2 Surface weather data	10
2.3 Upper-air data	13
2.4 Reanalysis data for weather charts	13
3. Characteristic of the occurrence	14
3.1 Temporal and spatial distributions of the occurrences	18
3.2 Classification of the vertical temperature profile	23
3.3 Ground surface temperature (GST) and surface air temperature (SAT)	26
4. Synoptic situation analysis	27
4.1 Classification of the 850-hPa geopotential field	30
4.2 Combining the 1000-hPa geopotential field with frontogenesis analysis	32
4.3 Classification of the 1000-hPa geopotential field with frontogenesis analysis	37
5. Forecasting tools	38
5.1 Thickness	41
5.2 Use of the p-type nomogram	43
5.3 Freezing rain detector (FRAD)	47
6. Summary and discussion	48
References	54
Acknowledgements	56

List of Figures

- Fig. 1.** Stations where the freezing precipitation was recorded: 24 stations (black circles) are KMA stations, 17 are North Korean (black crosses), and 7 are upper-air observation stations (grey triangles). Nine ROKAF stations were used, but their positions are not shown on the map. In Baeknyeongdo, near 38°N 124.7°E, the black circle and gray triangle overlap. 10
- Fig. 2.** The mean annual occurrence frequency of freezing precipitation. Black circles denote the station position. Nine ROKAF stations are not shown, but the data were included in the analysis. 15
- Fig. 3.** Mean annual frequencies (circle) of the freezing precipitation (the ww codes are 56, 57, 66, and 67) per station for 2001–2013. The dashed line is its trend curve. The number of piloted observation stations (vertical gray bar) and the records of freezing precipitation (vertical black bar) for each year are shown. 17
- Fig. 4.** The hourly (a) and monthly (b) occurrences of freezing precipitation. 18

Fig. 5. Vertical profiles of the temperature associated with the freezing level. a) ML-W denotes mid- and low-layer warm type, b) M-W does mid-layer warm type with two freezing levels, c) G-W is the ground-layer warm type, d) 3L-F is the 3-layer freezing type, e) W-P is the warm precipitation type, and f) CAD is the cold air-damming type. The characteristics of each type are described in the text. 23

Fig. 6. Same as Figs. 5a~f but for scatter diagrams between the ground surface temperature (GST) and the surface air temperature (SAT) for each type. g is the total. 26

Fig. 7. The representative cases of three categories of 850-hPa geopotential height fields when freezing precipitation occurred: (a) denotes the mid-level northwesterly wind (MNW) category, (b) the mid-level southerly wind (MS) category, and (c) the mid-level deformation (MD) category. 30

Fig. 8. The representative cases of six groups of the 1000-hPa geopotential height field with frontogenesis ($10^{-9} \text{ K S}^{-1} \text{ m}^{-1}$): a) denotes the warm-front group, b) the cold-front group, c) the cyclone rear-side group, d) the West Sea cyclone type, e) the anticyclone rear-side group, and f) the cold air-damming group. The inside white circle in the figure is the point the freezing precipitation occurred. 37

Fig. 9. The frequencies of the thickness values over a) 1000–850, b) 850–700, and c) 1000–500 thicknesses during freezing precipitation. 41

Fig. 10. a) P-type nomogram that the USA employs. b) Extended p-type nomogram used in this study. The FROA denotes the area where freezing rain is considered to be possible in the USA. A and B are areas of freezing precipitation that occurred in Korea, although it is the outward boundary of the USA p-type nomogram. Dots denote the occurrence of freezing precipitation. c) Same as in b), but for empty gray circles (data for 00, 06, 12, and 18 UTC from January 1 to February 28, 2014, Gwangju), d) two particular cases with extensive damage. The explanation is in the text. 44

Fig. 11. A device on the apparatus for the automatic detection of freezing rain. 46

List of Tables

Table 1. Five types of freezing-rain cases alongside the vertical temperature profile and the related occurrence frequency of each type. The frequencies of the shortest distances between the surface weather stations and the upper-air observing stations classified as 50-km intervals were added. (The exceptions are cases where both the GST and SAT readings were higher than 10 °C.)	12
Table 2. Frequencies alongside the classifications of 1000- and 850-hPa geopotential height patterns and vertical temperature profiles. All abbreviations are the same as those used in figures 5, 7, and 8 in this study. The three numbers with commas in (B) denote the frequencies alongside the classification in (A), in the order MNW, MS, and MD. (The exceptions are cases where both the GST and SAT are higher than 10 °C.)	28
Table 3. Comparison of mean of thickness values (gpm) of the freezing rain cases observed in other regions.	40

On the freezing precipitation in Korea and the basic schemes for its prediction

Sang-Hoon Kwon

Department of Environmental Atmospheric Sciences, the Graduate
school, Pukyong National University

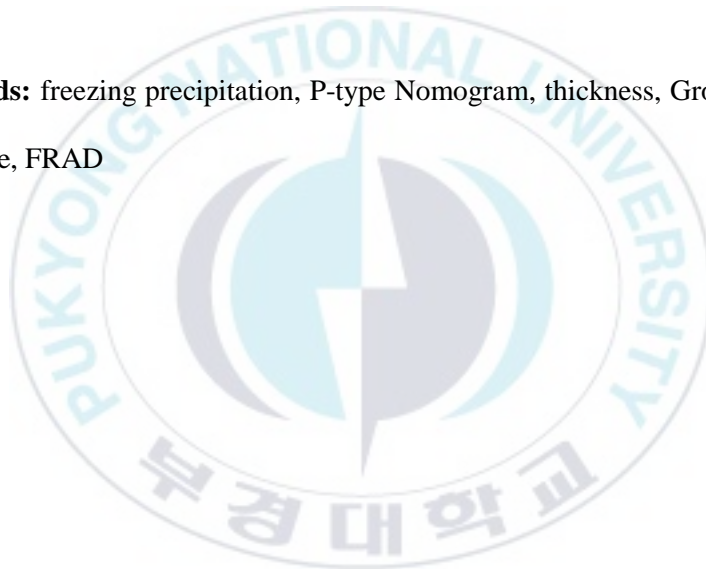
Abstract

This study aims to improve the forecasting skill for freezing precipitation. 102 freezing-precipitation cases were collected in South and North Korea from 2001 onward. Temperature fields on ground and atmosphere, vertical temperature profiles, geopotential fields, thicknesses fields and their spatiotemporal variations, and their combinations using the predominant-precipitation nomograms (p-type nomograms), were classified and investigated to determine whether these data could be used as predictors.

It was found that 1) the combination of the thicknesses of 1000–850-hPa and 850–700-hPa was a better parameter to be used to make p-type nomograms, which is very different from the one used in the USA, and 2) 35 groups on synoptic situations out of 72 are possible conditions for freezing precipitation, and 3) 3 groups out of 35, the 1000-hPa warm-front group, the mid-level southerly (MS) category of 850-hPa, and an mid-layer warm (M-W) type in the vertical temperature profile show the

greatest frequency. In spite of their increasing year-on-year trend, only a small part on freezing phenomena has been found until yet. The possibility of observation errors is the biggest problem. Additionally, the need for new equipment, the freezing rain detector (FRAD), to detect freezing precipitation automatically, is proposed. The denser observing system of FRADs and an ultra-fine gridded numerical model are suggested as a solution for the prediction of freezing precipitation.

Key words: freezing precipitation, P-type Nomogram, thickness, Ground surface temperature, FRAD



1. Introduction

Freezing rain denotes the rain of super-cooled water droplets that freeze as soon as they touch the ground surface, which is one form of natural disaster that can cause damage (Houston and Changnon, 2007). It causes traffic accidents and interruptions due to road-surface freezing, breakage of electric wires, forest damage, etc. (Brooks, 1920), and also induces aviation accidents due to ice attaching to the body aircraft in flight (Sand *et al.*, 1984; Pike, 1995; Ashenden and Marwitz, 1997). In practical terms, in the United States, the damage from freezing rain was US\$167 million between 1949 and 2000, which amounted to an average of US\$3.13 million per year (Changnon, 2003).

Around the world, especially in North America, the frequency of freezing rain is known to be high (Bennett, 1959), and much research has accumulated on the issue (McKay and Thompson, 1969; Gay and Davis, 1993; Stuart and Isaac, 1999; Cortinas, 2000). However, in other regions, documentation on this phenomenon is rarely found, although the damage incurred is suspected to be high. For Central Europe, a study has been conducted by Carrière *et al.* (2000); for Asia, studies have been conducted by Zhou *et al.* (2009), and Sun and Zhao (2010).

In the farming areas in Korea, freezing rain freezes autumn vegetables (e.g., radish and cabbage) so that they rot in the fields before harvest, or freezes fruits (e.g., apple and persimmon) so that they are damaged. In addition, traffic accidents occur

as a result of freezing rain (Kong et al., 2012). Despite the apparent damage, there is a tendency for freezing rain not to be viewed as a form of natural disaster. Therefore, very few studies on freezing rain have been undertaken in Korea. Kim *et al.* (2009) have produced extended abstracts for conferences as a related study, and Park and Byun (2014) paper is currently in the review process.

The mechanism for freezing precipitation has been classified into two categories: where super-cooled water droplets reach the ground surface just after the process of the melting of solid precipitation during falling and where super-cooled water droplets reach the ground surface in the process of freezing during the rain falling when they are not yet completely frozen. Solid precipitation melts during falling due to the effect of warm advection and the relevant physical processes are called the melting process (MP) (Brooks, 1920; Meisinger, 1920; Young, 1978; Stewart, 1985; Donaldson and Stewart, 1989; Gay and Davis, 1993; Martner *et al.*, 1993). During this process, the solid precipitation initially melts as it falls and then freezes again when it reaches the ground.

There is also a process called the super cooled warm rain process (SWRP), which involves a very thick cloud layer with a cloud-top temperature higher than -10°C . It is a process where super-cooled water droplets reach the ground surface without freezing because the ice nuclei are too small or there are no ice nuclei (Ohtake, 1963; Huffman and Norman, 1988; Rauber *et al.*, 2000, 2001). Park and Byun (2014) found a case in which falling rain is super-cooled as it encounters cold advection in the middle and lower layers of the atmosphere where these water

droplets reach the ground surface with an above-zero ground surface temperature (GST) and freeze while cooling the ground surface, and this is classified as the cold-advection type. However, this is only a simple and primitive explanation of the process, so we are in need of a more diverse and systematic classification.

According to the results of Steenburgh *et al.* (1997), Weber (1998), and Mireles *et al.* (2003), synoptic pressure patterns that form freezing rain are classified into three groups: the warm-front group, anticyclone rear-side group, and the cold air-damming (CAD) group. Among these, the warm-front group has drawn the most attention (Young, 1978; Donaldson and Stewart, 1989). It occurs most frequently in the right downwind side of a surface cyclone (i.e., the northern side of a warm front in the Northern Hemisphere). The CAD group mostly occurs on the downwind side of mountain ranges in the Northern Hemisphere, such as on the eastern coasts of the United States and Korea (Steenburgh *et al.*, 1997; Park and Byun, 2014). The anticyclone rear-side group requires further research, as the research is currently at a standstill (Mireles *et al.*, 2003).

The main purpose of most studies on freezing precipitation is to predict the occurrence of freezing rain in order to reduce damage. For this purpose, thickness has been widely used in previous studies. This is because thickness is proportional to the average virtual temperature of the layer. The 1000–700-hPa thickness (gpm) has been widely used to distinguish the forecasting of snow from rain. On the other hand, Gay and Davis (1993) and Heppner (1992) attempted to estimate precipitation patterns in advance by using the 1000–850-hPa and 850–700-hPa

thicknesses together. The predominant-precipitation nomogram (p-type nomogram) is the most commonly used method for predicting precipitation patterns (Keeter and Cline, 1991; Keeter *et al.*, 1995).

In this study, the temporal and spatial distributions of the occurrence of freezing rain in the Korean Peninsula during the period of 2001–2013 were organized, and the physical processes during occurrences, synoptic pressure patterns, vertical temperature profiles, and thickness distributions were classified and analyzed. This study also placed the emphasis on finding the reason as to why the technique used for freezing rain prediction was not sufficiently developed in the existing studies.

2. Data

2.1. On the observation and records

In general, freezing precipitation includes freezing rain (ZR) and freezing drizzle (ZL) (Stuart and Isaac, 1999). The basic principles of the two phenomena are the same, but it is classified as ZL when the diameter of a falling droplet is less than 0.5 mm, and as ZR when the diameter is more than 0.5 mm (Atmospheric Environment Service, 1977; Korea Meteorological Administration [KMA], 2002). However, Gay and Davis (1993) did not distinguish between the two phenomena and regarded them as freezing rain by including ZL in ZR.

Using the weather code numbers from code table 4677 of the International

Meteorological Code (IMC) developed by the World Meteorological Organization (WMO, 1995), ZL is recorded as 56 (light freezing drizzle) or 57 (moderate/heavy freezing drizzle), and ZR is recorded as 66 (light freezing rain) or 67 (moderate/heavy freezing rain) (WMO, 1995; Korean Meteorological Society and KMA, 2013). However, sleet and ice pellets are number 79 and are called frozen precipitation, which is different from hail in its size. These numbers are recorded every hour when they occur in the weather observation table (WOT) that is produced at every station each day, and are in the “ww” position in the WMO’s telegraph message (FM12 ~ FM14).

However, there are two problems in Korea with this form of data recording. The first is that ZR and ZL do not start or end within each hourly block, but they occur in the form of minutes. The start and end times are recorded not in the “ww” position but in the “Remarks” section of the WOT by an observer, who handwrites the findings. However, Korea (KMA, 2002) regulates that both the freezing rain (56, 57, 66, 67) and the ice pellets (79) are recorded as ‘❄’, which is the symbol for ice pellets. Therefore, the exact time of a freezing rain event cannot be discerned from an ice-pellet event by using the ‘Remarks’ section of the WOT. Therefore, this study depended only on the “ww” codes of the WOT.

The second issue in Korea is that freezing rain tends to occur consecutively before and after ice pellets or rain, and thus it is difficult to distinguish the time of the three phenomena from one another. Rain just after freezing rain erases the trace of freezing rain; thus, countless cases of freezing rain will have disappeared without

trace and without any human-observed records being made of the events. Cases of freezing rain events with no trace but with damage are only possible to note if they occur at night. These problems make it difficult to investigate freezing rain events in the Korean case. Some problems relating to terminology also exist. In the case of Korea, Hong (2013) translated “freezing rain” into “freezable rain.” It is hard to find international studies that do not distinguish precisely between freezing rain and other forms of solid precipitation.

Therefore, in this study, freezing rain was regarded to have occurred when the then current weather code (ww) was recorded as either 56, 57, 66, or 67, from November to May. Many cases of freezing rain will be omitted in this investigation (even though they were recorded) if an event occurred outside of an exact hour, but took place between one hour and the next.

2.2. Surface weather data

1) The surface air temperature (SAT), GST, and the weather with its code number (ww), which had been recorded every hour in the WOT of 77 locations provided by the KMA, were used. In Korea, meteorological data have been recorded at 1-hour intervals since May 5, 2001 (3-hour intervals had been used before May 5, 2001). Thus, in this study from May 5, 2001 to October 31, 2013, the hourly weather codes were used. A total of 46 freezing rain cases were

observed at 24 KMA stations out of 77.

In the case of the GST data, 1-hour-interval data are available from around 2008 for most stations. Before then, the data consisted of 6-hour-interval recordings. Therefore, the GST data at the times that were the closest to the occurrence time of freezing rain were used. Twenty-eight 6-hour-interval data items and 18 1-hour-interval data items were found and used.

2) Among the aeronautical meteorological observation data of 19 stations in Korea provided by the Republic of Korea Air Force (ROKAF), the hourly weather codes from May 5, 2001 to October 31, 2013, which is the same period as that of the KMA, were used. A total of 14 freezing rain cases were observed at 9 stations out of 19. These data have no GST information or remarks. As these are military stations, we have not pointed them out on the map, but the data are used in the calculations.

3) The 3-hour-interval observation data of 27 stations in North Korea from May 5, 2001 to October 31, 2013 were used. It is not known whether observations are made every hour in North Korea, but they transmit their meteorological observation data to China and Japan at 3-hour intervals following the WMO regulations. These data have no GST information or remarks. A total of 42 freezing rain cases were found at a total of 17 stations out of 27.

4) Among a total of 123 manned stations used in this study, the number of locations where freezing rain was observed once or more was 50 (Fig. 1).

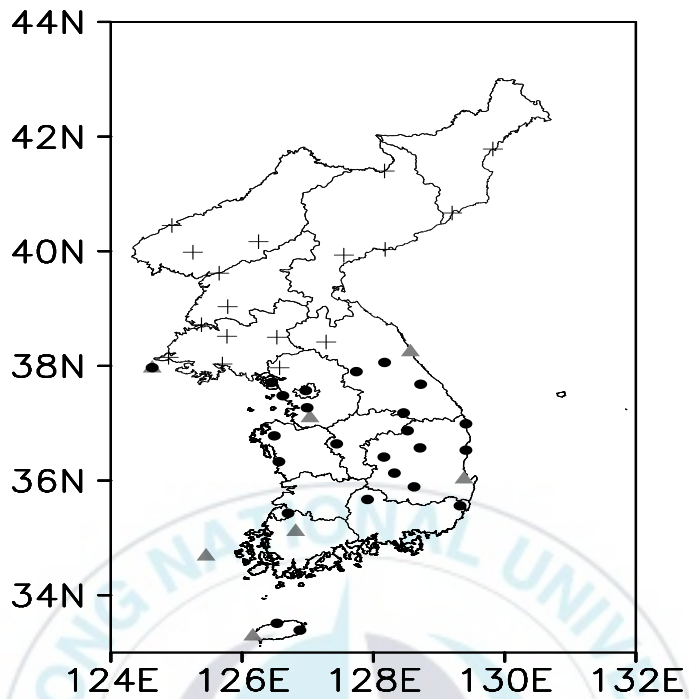


Fig. 1. Stations where the freezing precipitation was recorded: 24 stations (black circles) are KMA stations, 17 are North Korean (black crosses), and 7 are upper-air observation stations (grey triangles). Nine ROKAF stations were used, but their positions are not shown on the map. In Baeknyeongdo, near 38°N 124.7°E, the black circle and gray triangle overlap.

2.3. Upper-air data

1) Rawinsonde data (air temperature) from seven stations in Korea (Osan (47122), Gwangju (47158), Baeknyeongdo (47102), Heusksando (47169), Jeju (47185), Pohang (47138), and Sokcho (47090)) with 6- or 12-hour intervals, provided by Wyoming University (<http://weather.uwyo.edu/upperair/sounding.html>), were used. From a total of 123 stations, the nearest station and closest in time out of 7 rawinsonde stations were decided on and were named as the substitution points. Two example cases of the substitution points are explained below. One is when the freezing rain occurred at the same time but at another station (Seoul, 1700 KST [Korean standard time], January 12, 2006; Incheon, 1700 KST, January 12, 2006). In this case, the nearest station (substitution point) is Osan. Then the rawinsonde data of Osan (0000 UTC, January 12, 2006) were used. The other cases are the continuous occurrences such as at Ulsan (1800 and 1900 KST, February 11, 2005). In these cases, the data from Pohang (1200 UTC, February 11, 2010) were used because the closest time is 1200 UTC. Therefore, although 102 cases of freezing rain were observed, 64 cases of rawinsonde data were used. (KST is 9 hours earlier than UTC.) The distances between the main stations and the substitution points are shown in Table 1. The mean distance is 120 km, with a standard deviation of 96 km, and the longest is 400 km, caused by the fact that North Korea has no rawinsonde stations.

TABLE 1. Five types of freezing-rain cases alongside the vertical temperature profile and the related occurrence frequency of each type. The frequencies of the shortest distances between the surface weather stations and the upper-air observing stations classified as 50-km intervals were added. (The exceptions are cases where both the GST and SAT readings were higher than 10 °C.)

Type	Freq.	Sonde data	Distance (50-km range)								
			1	2	3	4	5	6	7	8	9
ML-W	37	23	2	10	10	3	1	6	0	4	1
M-W	20	6	11	5	4	0	0	0	0	0	0
G-W	21	17	3	7	6	0	4	1	0	0	0
3L-F	7	5	1	3	2	0	0	0	0	0	1
W-P	7	5	0	3	0	0	4	0	0	0	0
CAD	5	3	0	3	2	0	0	0	0	0	0
Exception	5	5	1	3	0	1	0	0	0	0	0
Total	102	64	18	34	24	4	9	7	0	4	2

2) The thickness was analyzed using the data from the Modern Era Retrospective Analysis for Research and Applications (MERRA) provided by the National Aeronautics and Space Administration (NASA). These data have an interval of 6 hours and a grid spacing of $0.5^\circ \times 0.5^\circ$, and consist of 42 layers. Among them, the geopotential height data of four layers (1000, 850, 700, and 500-hPa) were used. The substitution points were decided on as for the rawinsonde data, but for the closest position of the grid point.

2.4. Reanalysis data for weather charts

1) The final (FNL) global-analysis filed data provided by the Global Data Assimilation System (GDAS) of the National Centers for Environmental Prediction (NCEP, <http://rda.ucar.edu/datasets/ds083.2/>) were used. The data consist of 26 layers from 1000-hPa to 10-hPa, cover the full globe with $1.0^\circ \times 1.0^\circ$ grids, and provide state-of-the-art homogeneous filed data every 6 hours. In this study the air temperature, u-vector, v-vector, and geopotential height data of two layers were used (1000 and 850-hPa).

3. Characteristic of the occurrence

3.1. Temporal and spatial distributions of the occurrences

Figure 2 shows the occurrence frequency of freezing precipitation for each location. It is the highest at Baeknyeongdo ($0.46 \text{ cases year}^{-1}$), an island located over the West Sea near 38°N , and 19 stations had the same value ($0.077 \text{ cases year}^{-1}$) as their lowest frequency. Notably, the occurrence frequency is higher in North Korea. However, it is very hard to deduce other characteristics from this figure, which means the recorded cases are not sufficient enough to find some of the trends, as explained in section 2-1.

Figure 3 shows the annual occurrences of freezing precipitation, and those divided by the number of total manned stations for the corresponding year, which represents the average occurrence frequency of freezing precipitation that occurred during a year at a particular location. The number of manned observation locations decreased between 2008 and 2009; but during the entire 13-year period, the occurrence frequency of freezing precipitation at each location showed a gradually increasing trend. It was in the order of 2012 ($0.28 \text{ cases station}^{-1}$), 2006 ($0.22 \text{ cases station}^{-1}$), and 2009 ($0.15 \text{ cases station}^{-1}$).

It is estimated that the increase of the occurrence frequency is due to the development of observation technology, rather than to any actual increase of the occurrences.

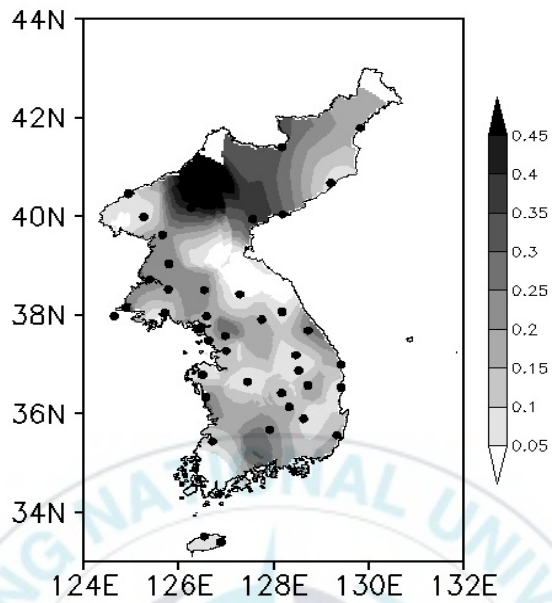


Fig. 2. The mean annual occurrence frequency of freezing precipitation. Black circles denote the station position. Nine ROKAF stations are not shown, but the data were included in the analysis.

For the occurrence time, 0900 KST had the highest frequency (Fig. 4a), 1800 KST had the second, and three time zones (1200, 1500, and 2400 KST) had the third highest frequency. It is presumed that ground surface cooling in the morning and convection intensification in the afternoon affected the occurrence of freezing precipitation, but there was a time delay during the development of convection. However, another guess is that 0900 and 1800 KST are the times when the observing activity is the most active. In other words, many freezing-precipitation events were not recorded due to the failure in observation. In addition, it is clear that there were cases where freezing precipitation occurred due to synoptic circulation besides the above two cases. When it was due to synoptic circulation, the occurrence time was not limited to a specific time. In addition, the frequency was in the order of February (26 cases), January (24 cases), and December (21 cases); and it was the lowest in October (twice) (Fig. 4b).

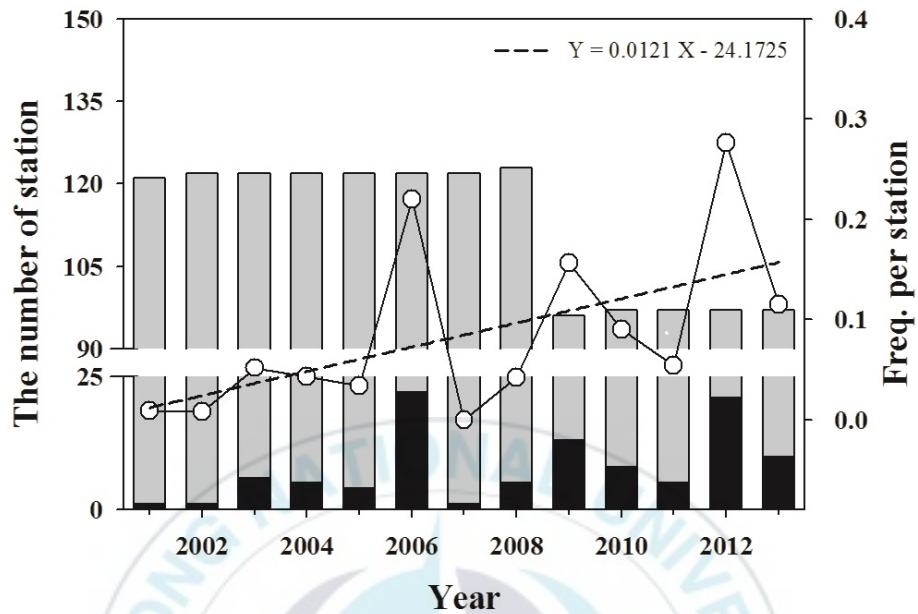


Fig. 3. Mean annual frequencies (circle) of the freezing precipitation (the ww codes are 56, 57, 66, and 67) per station for 2001–2013. The dashed line is its trend curve. The number of piloted observation stations (vertical gray bar) and the records of freezing precipitation (vertical black bar) for each year are shown.

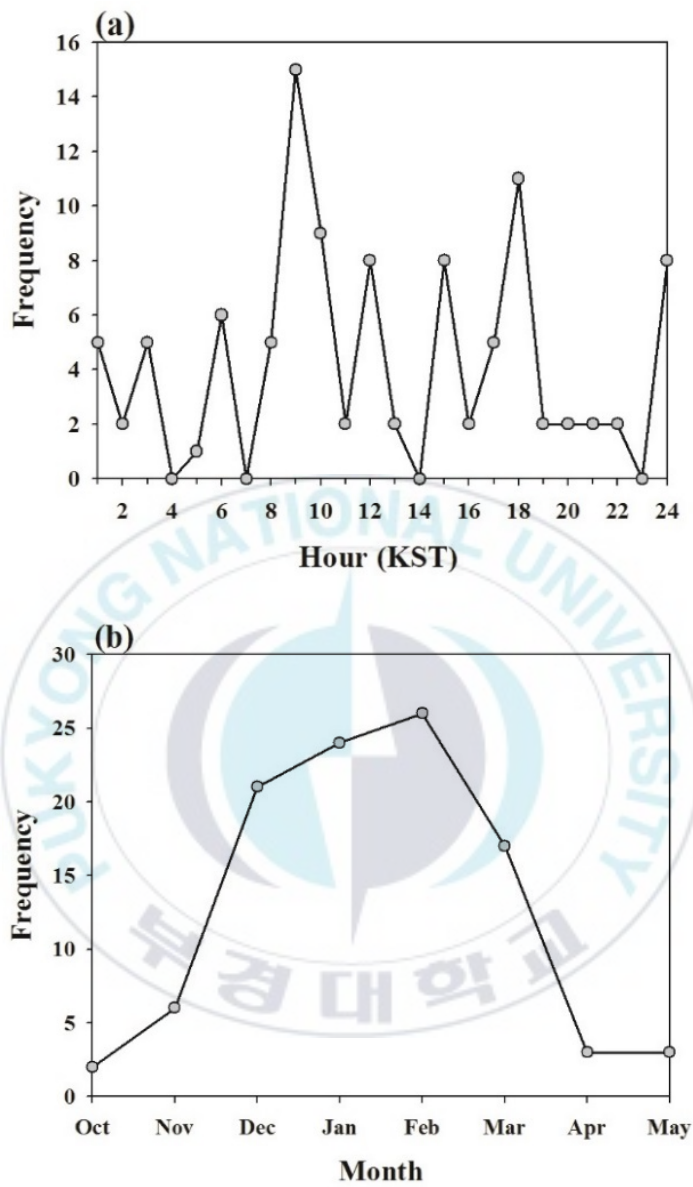


Fig. 4. The hourly (a) and monthly (b) occurrences of freezing precipitation.

3.2. Classification of the vertical temperature profile

As shown in figure 5, vertical temperature profiles were classified into six types. Each of the types are explained next. The gray lines represent the vertical temperature profiles that correspond to the types and the black lines represent the average air temperatures of the standard heights (1000, 925, 850, 700, and 500-hPa). The frequencies of each type are summarized in Table 1.

(1) Mid- and low-layer warm (ML-W) type

In figure 5a, the freezing levels are higher than 900-hPa. Thus, it was named the mid- and low-layer warm (ML-W) type. In this study, the height above 900-hPa is called the middle layer to distinguish it from the ground level. It is where the solid precipitation of the middle and upper layers melts near the ground and reaches the ground. The frequency with this type was the highest (42 cases). However, as 5 of these cases are above 10 °C in both the GST and SAT readings, only 37 cases were involved in this group, and the analysis involved the 23 different rawinsonde data items. The five excluded cases were two KMA and three North Korean cases. It is expected that the surrounding air temperature rises due to the latent heat released when freezing precipitation reaches the ground level and freezes. In practice, Stallabrass (1983) reported that the SAT increased by 0.3 °C hour⁻¹ during freezing precipitation. However, this cannot raise the GST or SAT levels up to 10 °C.

In these cases, it is questionable whether there was no error during the observation. Therefore, these five cases (KMA: 2, North Korea: 3) have been excluded from further analysis.

(2) Mid-layer warm (M-W) type

Figure 5b is similar to figure 5a, but is different in that there were two freezing levels. The air temperature of the bottommost layer was below zero (near 0 °C). Two freezing levels were observed because an air layer with an above-zero temperature was formed in the middle of the troposphere due to the warm advection. It is the most well-known type, where solid precipitation that has frozen in the upper layer completely melts as it passes the warm layer, cools again as it passes the cold layer near the ground, and freezes as it reaches the ground surface. Twenty cases were observed, but using the six different rawinsonde data items, and it was named as the mid-layer warm (M-W) type.

(3) Ground-layer warm (G-W) type

In figure 5c, there was one freezing level, and it was below 900-hPa. This is the case where solid precipitation completely melts as it passes the surface layer with an above-zero temperature, but the liquid reaches the ground surface still having a below-zero temperature. It is thought that the liquid maintains a below-zero temperature due to continuous heat loss during repeated melting and evaporation. Thus, it was named the ground-layer warm (G-W) type, and 21 cases were

observed, but using the 17 different rawinsonde data items.

(4) 3-Layer freezing (3L-F) type

Figure 5d shows the case with three freezing levels. In this case, the ground layer has an above-zero temperature. In the middle layer, precipitation freezes, melts, and freezes again; and then it melts again due to the warm air of the surface and reaches the ground surface. It is not clear whether it actually consists of repeated freezing and melting. It was named the 3-layer freezing type (3L-F), and seven cases were observed, but using the five different rawinsonde data items.

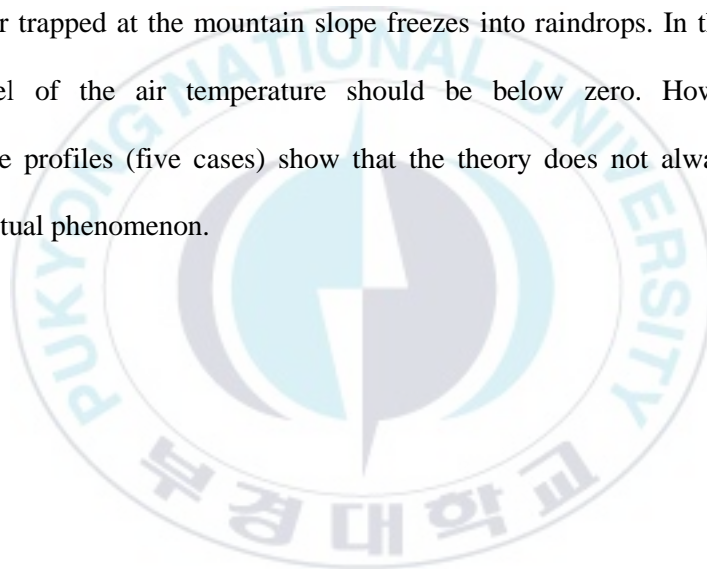
(5) Warm precipitation (W-P) type

Figure 5e shows that the air temperatures of the whole layers were below zero, but most of them were near 0 °C. In the upper layer, there was a layer that was close to 0 °C, but a colder layer was located just below that layer. The formation processes can be classified into two cases. In the first case, the SWRP is formed in the upper layer, but precipitation falls while cooling as cold advection occurs in the middle layer. In the second case, an original air layer is cold, but warm advection occurs in the upper layer. This completely melts precipitation particles, which have already been formed, in the upper layer, and then they fall. Therefore, warm advection in the upper layer (or cold advection in the middle layer) is thought to be the major cause. It was named the warm precipitation type (W-P), and seven cases were

observed, but using the five different rawinsonde data items.

(6) Cold air-damming (CAD) type

On the eastern slope of the Taebaek Mountains, the phenomenon of the CAD type is known to be frequent. Three stations at Ulsan, Uljin, and Yeongdeuk are located in this area and five cases of the events were drawn, as shown in figure 5f, but using the three different rawinsonde data items. It is easy to imagine a process were the cold air trapped at the mountain slope freezes into raindrops. In this case, the lower level of the air temperature should be below zero. However, three temperature profiles (five cases) show that the theory does not always coincide with the actual phenomenon.



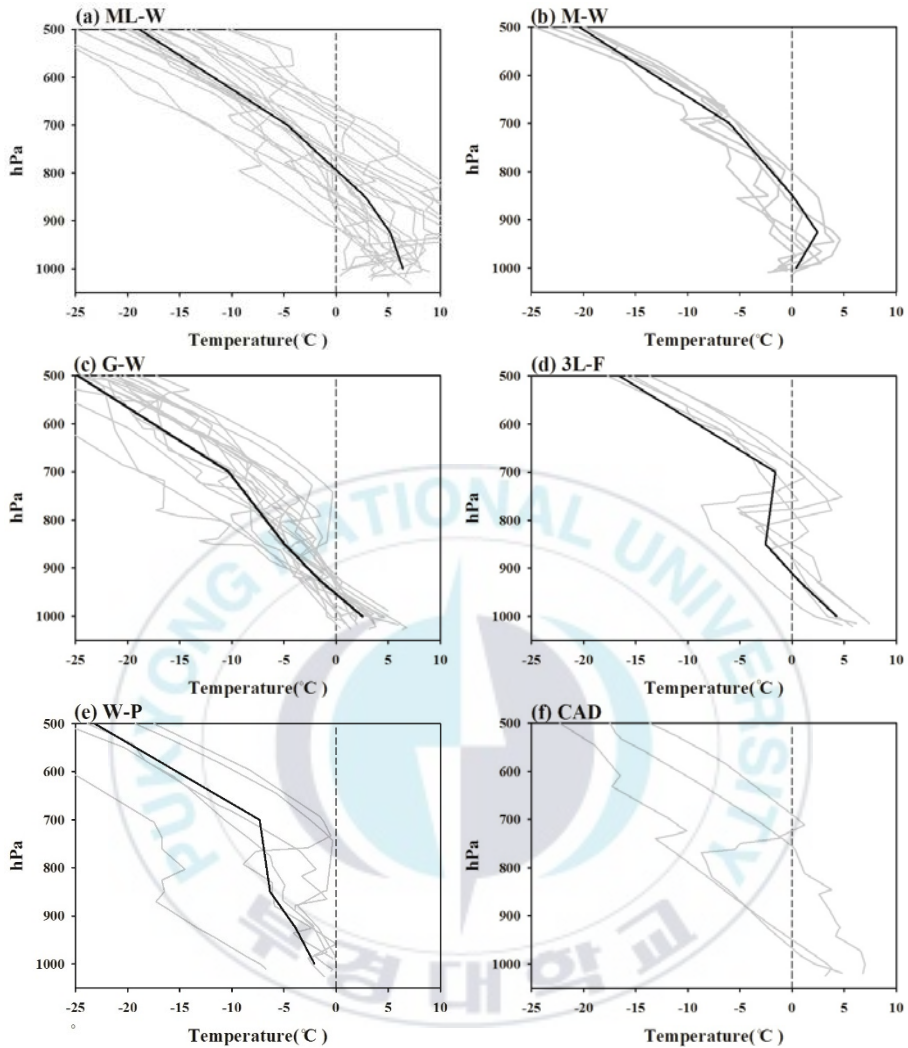


Fig. 5. Vertical profiles of the temperature associated with the freezing level. a) ML-W denotes mid- and low-layer warm type, b) M-W does mid-layer warm type with two freezing levels, c) G-W is the ground-layer warm type, d) 3L-F is the 3-layer freezing type, e) W-P is the warm precipitation type, and f) CAD is the cold air-damming type. The characteristics of each type are described in the text.

3.3. Ground surface temperature (GST) and surface air temperature (SAT)

In general, it is known that freezing precipitation occurs when the GST (Djuric, 1994) or SAT (Gay and Davis, 1993) is below 0 °C. However, this study shows different results. Figures 6a–e show the relation between the GST and the SAT for each type in figures 5a–e. Here, the GST and SAT of the ROKAF stations and North Korean stations (totaling 56 cases) were excluded because they were not observed the GST. The two cases in Korea were excluded because both the GST and SAT were above 10 °C, as mentioned previously. In figure 6g, 21 cases above zero in SAT and GST can be seen. These are the cases belonging to a, c, d, and f in figures 5 and 6. It is still hard to understand why they freeze. The ground is too warm to be frozen. The reason for this discordance may come from the difference in the observing time. The GSTs were measured every hour or every 6 hours, but freezing precipitation sometimes persists for only a few minutes. Most of these cases are a type of ML-W (Fig. 6a). The temperatures in cases of M-W and W-P are concentrated near zero. Only in 15 cases was the SAT above zero and the GST below zero. These are the cases where falling droplets freeze on reaching the ground, as Rauber *et al.* (2001) pointed out. One important thing to be noted in this figure is that the GST is more concentrated than the SAT, therefore it is more appropriate to use for forecasting than the SAT (Fig. 6f). GSTs were distributed

between $-2-4$ °C. Forty cases (91%) were within the range of $-1-2$ °C, and the average GST was 0.35 °C. SATs were distributed between $-2.7-5.7$ °C, 40 cases (91%) were within the range of $-1.7-3.5$ °C, and the average SAT was 1.21 °C.



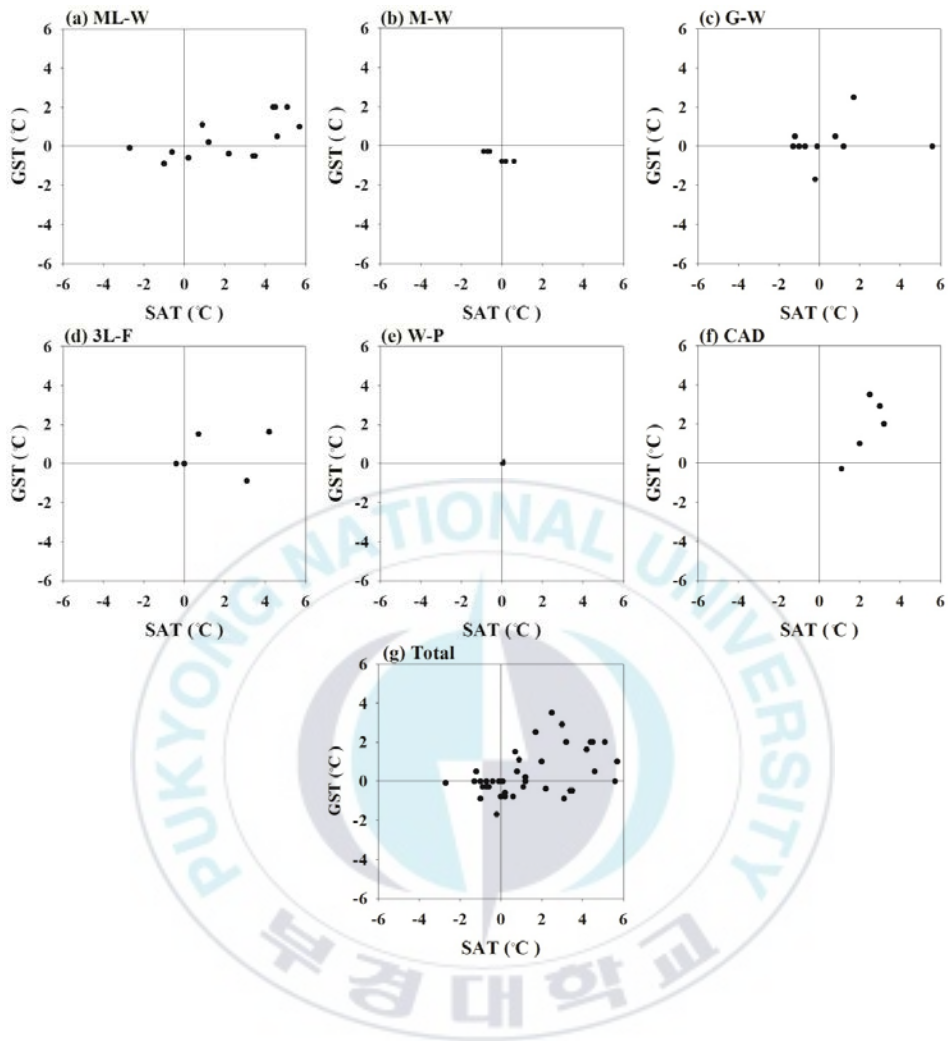


Fig. 6. Same as Figs. 5a~f but for scatter diagrams between the ground surface temperature (GST) and the surface air temperature (SAT) for each type. g is the total.

4. Synoptic situation analysis

4.1. Classification of the 850-hPa geopotential field

As most of the meteorological phenomena occur with a characteristic pressure pattern, a classification of pressure fields associated with freezing precipitation is needed. There are two common-sense ideas on the pressure fields that form freezing precipitation. Firstly, it is the pressure fields that can produce rain or snow; in other words, they are related to a low pressure system or trough etc. Secondly, in these pressure fields, the vertical profile of the air temperature is around freezing point, as explained earlier. Thus, not all winter rains accompany freezing precipitation. Five cases are excluded because both the GST and SAT readings were above 10 °C, as discussed in section 3-2-(1). Therefore, 97 cases out of 102 were classified into three categories in the 850-hPa geopotential height field. Firstly is the mid-level northwesterly (MNW) category (Fig. 7a), where the inflow of cold northwesterlies from the high latitudes intrudes. These northwesterlies are not the real wind, but the suspected wind from the pressure gradient. Though 34 cases were included in this category (Table 2), it is not always a case of cold air. Classifications along the vertical profile—warm air at the middle and low layer (ML-W type, 12 cases) and at mid layer (M-W type, 1 cases), although they are the opposite concept to MNW—are included in this category. The G-W (11 cases), 3L-F (5 cases), and W-P type (5 cases) are also in this category.

TABLE 2. Frequencies alongside the classifications of 1000- and 850-hPa geopotential height patterns and vertical temperature profiles. All abbreviations are the same as those used in figures 5, 7, and 8 in this study. The three numbers with commas in (B) denote the frequencies alongside the classification in (A), in the order MNW, MS, and MD. (The exceptions are cases where both the GST and SAT are higher than 10 °C.)

6 Groups and extra. in 1000-hPa	Freq.	3 categories of the 850-hPa geopotential field (A)			6 types of vertical temperature profile (B)					
		MNW	MS	MD	ML-W	M-W	G-W	3L-F	W-P	CAD
Warm-front	39	8	28	3	0,10,2	0,11,0	2,5,1	4,1,0	2,1,0	-
Cold-front	12	12	0	0	4,0,0	1,0,0	5,0,0	0,0,0	2,0,0	-
Cyclone rear-side	7	7	0	0	4,0,0	0,0,0	2,0,0	0,0,0	1,0,0	-
West Sea cyclone	6	3	1	2	2,1,2	0,0,0	1,0,0	0,0,0	0,0,0	-
Anticyclone rear-side	21	4	16	1	2,9,1	0,7,0	1,0,0	1,0,0	0,0,0	-
Cold air-damming	5	0	3	2	-	-	-	-	-	5
Unclassified	7	-	-	-	-	1	4	1	1	-
Exception Cases	5	-	-	-	5	-	-	-	-	-
Total	102	34	48	8	42	20	21	7	7	5

Secondly, the mid-level southerly (MS) category shows the inflow of warm air from the low latitudes to Korea (48 cases, Fig. 7b). Classifications along the vertical profile—cold air at the middle layer (GW type: 5 cases, 3L-F type: 1 case and WP type: 1 case) although they are the opposite concept to MS are included in this category. But the ML-W (20 cases), M-W (18 cases) are highest in this category. The remaining 3 cases were included the CAD type.

Thirdly, the mid-level deformation (MD) category has a deformation field that is located around Korea (8 cases, Fig. 7c). Five out of eight cases belonged to the ML-W type. The remaining seven cases were hard to incorporate into the above three categories. Though we succeeded in classifying the 850-hPa geopotential height field, attempts to find some beneficial clues relating the 850-hPa geopotential height field to the vertical temperature still require further consideration. The fact that pressure-field classification involves many subjective factors is one of the reasons for this.

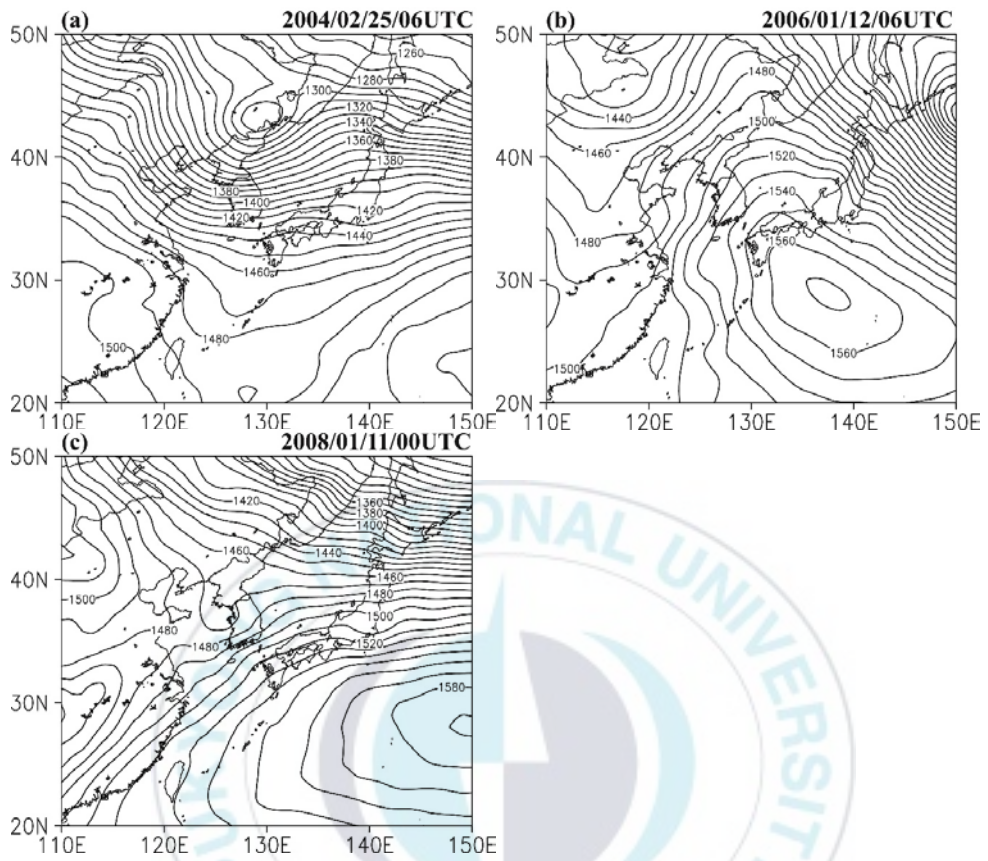


Fig. 7. The representative cases of three categories of 850-hPa geopotential height fields when freezing precipitation occurred: (a) denotes the mid-level northwesterly wind (MNW) category, (b) the mid-level southerly wind (MS) category, and (c) the mid-level deformation (MD) category.

4.2. Combining the 1000-hPa geopotential field with frontogenesis analysis

Freezing precipitation is related to rain or snow and most events are correlated with a low, a trough, or a front in the surface weather chart. The front near-surface level is the most important factor in terms of producing precipitation. Therefore, the frontogenesis of the surface weather chart for the freezing-precipitation cases was carried out. Though Rauber *et al.* (2001) classified only the surface weather chart of the freezing-precipitation cases, this study was aided by the frontogenesis results.

Analyses of frontogenesis were carried out through this process using eq. (1), defined by Petterssen (1936).

$$(1) \quad \mathbf{F} \text{ (frontogenesis)} = \frac{d}{dt} |\nabla_h \theta|$$

where \mathbf{F} is the frontogenesis function. Keyser *et al.* (1988) simplified the equation by resolving \mathbf{F} into natural coordinates (\mathbf{s} , \mathbf{n}) such that the \mathbf{s} axis is locally tangential to isentropes and the \mathbf{n} axis points toward colder air on a constant pressure surface.

$$(2) \quad \mathbf{F} = F_n \mathbf{n} + F_s \mathbf{s}$$

$$(3) \quad F_n = -\frac{d}{dt} |\nabla_h \theta| = -|\nabla_h \theta|^{-1} \left[\frac{\partial \theta}{\partial x} \left(-\frac{\partial u}{\partial x} \frac{\partial \theta}{\partial x} - \frac{\partial v}{\partial x} \frac{\partial \theta}{\partial y} \right) + \frac{\partial \theta}{\partial y} \left(-\frac{\partial u}{\partial y} \frac{\partial \theta}{\partial x} - \frac{\partial v}{\partial y} \frac{\partial \theta}{\partial y} \right) \right]$$

$$(4) \quad F_s = \mathbf{n} \cdot \left(\mathbf{k} \times \frac{d}{dt} \nabla_h \theta \right) = -|\nabla_h \theta|^{-1} \left[\frac{\partial \theta}{\partial y} \left(-\frac{\partial u}{\partial x} \frac{\partial \theta}{\partial x} - \frac{\partial v}{\partial x} \frac{\partial \theta}{\partial y} \right) - \frac{\partial \theta}{\partial x} \left(-\frac{\partial u}{\partial y} \frac{\partial \theta}{\partial x} - \frac{\partial v}{\partial y} \frac{\partial \theta}{\partial y} \right) \right]$$

$$(5) \quad \nabla_h = \mathbf{i} \frac{\partial}{\partial x} + \mathbf{j} \frac{\partial}{\partial y}$$

Here, ∇_h is the horizontal gradient operator, F_n refers to changes in magnitude of the thermal gradient, and F_s refers to the changes in direction of the thermal gradient with no magnitude change (Keyser *et al.*, 1988). If the calculated value is positive, frontogenesis is implied in the actual atmosphere; and a negative value indicates the implied frontolysis.

Thus, for the 97 cases of freezing precipitation, combined 1000-hPa geopotential height fields with their respective frontogenesis calculations were prepared. They were classified into six groups: the warm-front group, cold-front group, cyclone rear-side group, West Sea cyclone group, anticyclone rear-side group, and the CAD group. They are explained below with representative cases, as shown in figure 8.

There are substantial problems with these weather data. FNL data are for 6-hour intervals. Vertical temperature profile data are for 6- or 12-hour intervals. Meteorological observations of the surface layer such as SAT, GST, and the weather are at 1- or 3- or 6-hour intervals. Traveling speeds of the weather systems should also be considered. For example, the cold front normally moves at 5–15 km per hour. Moreover, the spatial distance from the surface weather stations to the upper-air observing station is not close enough, as shown in Table 1. However, more precise data are not available when many cases of freezing precipitation are examined. Therefore, attempts to predict the occurrence of freezing precipitation should be continued in spite of these problems.

4.3. Classification of the 1000-hPa geopotential field with frontogenesis analysis

(1) Warm-front group

The warm-front group is where freezing precipitation occurs at the front side of a warm front (Fig. 8a) and the low is located over the sea. Park and Byun (2014) used the same terminology. Thirty-nine cases were observed, which had the highest occurrence. It was found that warm fronts strongly developed around the southern coast of Korea.

This group is related to all of the three categories classified by the 850-hPa geopotential height field, but MS (Fig. 7b) is the most frequent category (28 cases). Two kinds of freezing processes are presumed to occur in this category. The first is where snow falling from the upper layer melts due to the warm layer formed in the middle layer and is cooled again near ground. The second is where rain formed in the mid-layer is cooled near the surface layer. Therefore M-W (11 cases) and ML-W (10 cases) both have more cases than for G-W (5 cases) (Table 2). Though the combination of 1000-hPa warm fronts and 850-hPa northwesterlies (MNW in Fig 7a) is hard to imagine, eight cases, with four cases of the 3L-F type, were detected, which means that there was a very complicated vertical structure with three freezing levels. The MD (Fig. 7c, 3 cases) is a case where the location of the freezing-precipitation occurrence is situated at the axis of the outflow of the deformation field. This is where precipitation is formed as the warm air from the

low latitudes and the cold air from the high latitudes meet each other.

(2) Cold-front group

Twelve cases were observed at the rear side of a cold front and were called the cold-front group (Fig. 8b). Unlike the warm-front group, freezing precipitation is formed at the rear side of a cold front stretching out from the low located at the eastern part of the Asian land. The cold air from the high latitudes moves underneath the warm air from the low latitudes. This group appeared only in MNW (Fig. 7a). In this regard, the role of cold advection is to super-cool falling droplets. However, the vertical temperature profiles show that there are G-W (5 cases), ML-W (4 cases), W-P (2 cases), and M-W (1 case) types. For the cold front, the change in the precipitation pattern is in the order of rain, freezing precipitation, ice pellets, and snow, which is the opposite of the change in the precipitation pattern occurring in a warm front (Martner *et al.*, 1993). Consequently, it is difficult for a cold front with a 1000-hPa and a G-W in the vertical temperature profile to occur at the same time. These issues have already been discussed in section 4-2.

(3) Cyclone rear-side group

There were seven cases belonging to the cyclone rear-side group (Fig. 8c). The characteristic of this group is the location of the low, which is in the northern part of the East Sea. This group appeared only in the MNW category (Fig. 7a). The major part of this group belongs to the ML-W type (4 cases). In this group, low-

level flows are not through an easterly or northeasterly wind, but through a mid-level northwesterly wind, which means the backing of a vertical wind shear; in other words, cold advection.

(4) West Sea cyclone group

In the West Sea cyclone group (Fig. 8d, 6 cases), the distinct development of a warm front is not observed. That is different from the warm-front group. Over the West Sea, a low or a trough from the low located over the Eastern China Sea is found. The warm southeasterly in low level current to Korea is the main cause of the freezing rain. . Thus, the ML-W type (5 cases out of 6) is the main finding.

(5) Anticyclone rear-side group

In the anticyclone rear-side group (Fig. 8e, 21 cases), freezing precipitation is formed at the rear side of an anticyclone as a southeasterly supplies the warm air. In this group, the MS category (Fig. 7b, 16 cases) and ML-W (9 cases) category are the most frequent because of the southerlies. The specific differences from the other types are due to the location of the low that is far from Korea, while the high is strong over Korea, and no fronts are seen over Korea.

(6) Cold air-damming group

The freezing precipitation of the CAD group is formed as a warm advection over the cold air trapped in the lower layer due to topographic factors. On the eastern

coast of Korea, it is mostly formed by easterlies. Unlike the Appalachian Mountains in North America, the distance between the top of the Taebaek Mountains and the East Sea is not far, at only 16 km at the narrowest point. Therefore, for the CAD group on the eastern coast of Korea, unlike North America, this type of event is seldom observed and noted on the weather chart, and it is very difficult to understand the correlations with the other vertical profile types, as mentioned in section 3-2-(6). Additionally, only very few studies have been carried out to date.



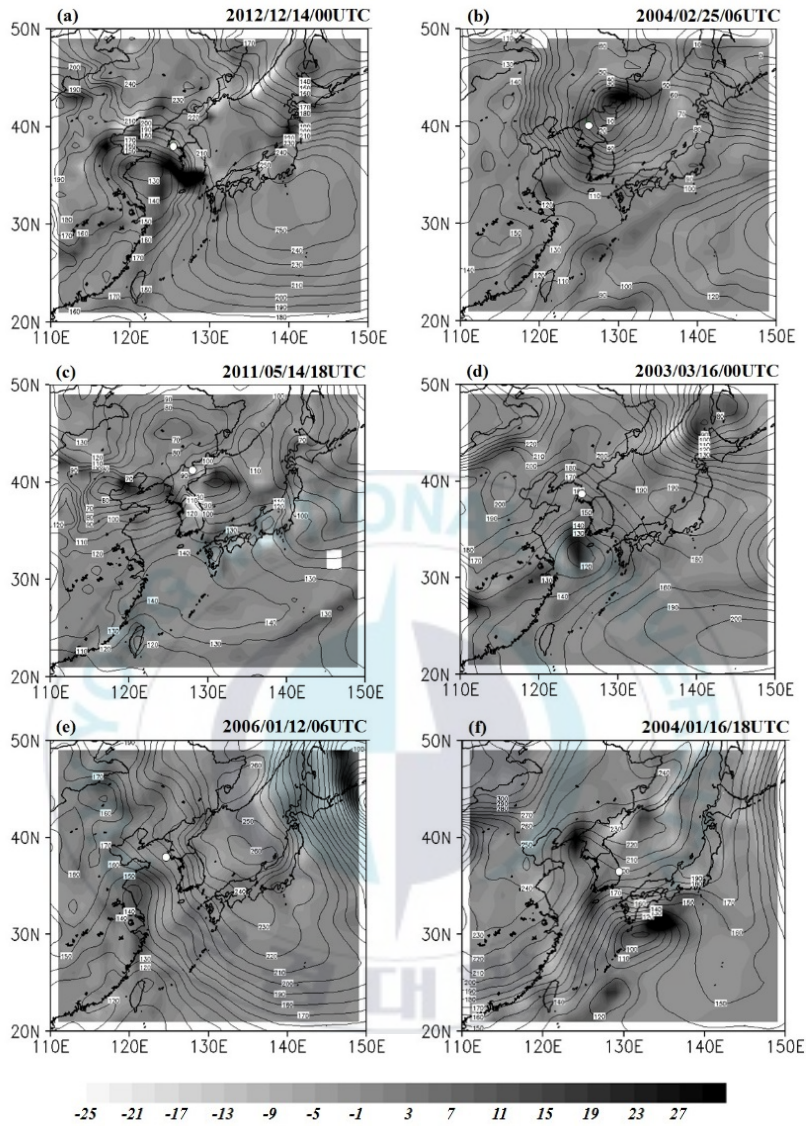


Fig. 8. The representative cases of six groups of the 1000-hPa geopotential height field with frontogenesis ($10^9 \text{ K S}^{-1} \text{ m}^{-1}$): a) denotes the warm-front group, b) the cold-front group, c) the cyclone rear-side group, d) the West Sea cyclone type, e) the anticyclone rear-side group, and f) the cold air-damming group. The inside white circle in the figure is the point the freezing precipitation occurred.

5. Forecasting tools

5.1. Thickness

Thickness has large effects on whether the precipitation pattern on the ground will be snow or rain (Gay and Davis, 1993). Eq. (6) explains the thickness (h)

$$(6) \quad h = \frac{R_d \bar{T}_v}{g_0} \ln \left(\frac{P_1}{P_2} \right)$$

where R_d represents the gas constant of dry air ($287 \text{ J kg}^{-1} \text{ K}^{-1}$), g_0 represents the gravitational acceleration (9.8 m s^{-2}), and P_1 and P_2 represent the atmospheric pressures of the upper isobaric surface and the lower isobaric surface, respectively. This equation indicates that thickness is proportional to the average virtual temperature \bar{T}_v of the two pressure surfaces, P_1 and P_2 . In other words, thickness represents the temperature of the layer through which falling precipitation passes. If it is above zero, snow melts; and if it is below zero, raindrops freeze. In theory, if the thickness of the atmospheric layer with an above-zero temperature is more than 300 m, snow completely melts during falling. Additionally, if the thickness of the atmospheric layer with a below-zero temperature is more than 400 m, falling droplets completely freeze (Djuric, 1994). Therefore, it has been widely used for the forecasting of precipitation patterns. The ultimate goal of this study is also the forecasting of freezing precipitation, and thus thickness is examined. This is because the prediction of freezing precipitation would be very difficult if based only on the classification of the vertical structures of atmospheric layers or the

classification of weather charts.

For the 97 freezing-precipitation cases that were observed in Korea, the average values for the three kinds of thicknesses (1000–850, 850–700, and 1000–500-hPa) were calculated to be 1308 m, 1533 m, and 5403 m, respectively. These values are smaller than the one suggested by Heppner (1992) or Koolwine (1975), but higher than the one by Rauber *et al.* (2001) in the lower level, and they were lower in the higher level, as seen in Table 3. In other words, the average values of the thicknesses that form freezing precipitation vary depending on the target region of each study.

Figure 9 shows the distribution of the thickness values during freezing precipitation. The maximum frequencies were observed at 1305–1310 gpm (Fig. 9a), at 1545–1550 gpm (Fig. 9b), and at 5420–5440 gpm (Fig. 9c), respectively. In addition, they had the ranges of 1265–1375 gpm (width = 110), 1475–1580 gpm (105), and 5170–5560 gpm (390), respectively. Especially, the thickness range of 1000–500-hPa was too wide, and it was found to be inappropriate for forecasting factors. For the 1000–850 thickness, 89 cases (92%) were within the range of 1280–1330 gpm, and for the 850–700 thickness, 88 cases (91%) were within the range of 1495–1560 gpm.

In figure 9, most of the points that are outside the concentrated area were the cases recorded in North Korea. This problem seems to have happened due to the long distance between the surface weather observation stations and the upper-air observation stations, as shown in Table 1 and section 2-3.

TABLE 3. Comparison of mean of thickness values (gpm) of the freezing rain cases observed in other regions.

Thickness layer (hPa)	Classification			
	This study (Standard dev.)	Albany, US (Heppner, 1992)	Ontario, Canada (Koolwine, 1975)	US East of Rocky Mountains (Rauber <i>et al.</i> , 2001)
1000–850	1308 (16)	1317	1313	1300
850–700	1533 (20)	1559	1539	-
1000–500	5403 (72)	5465	-	5456



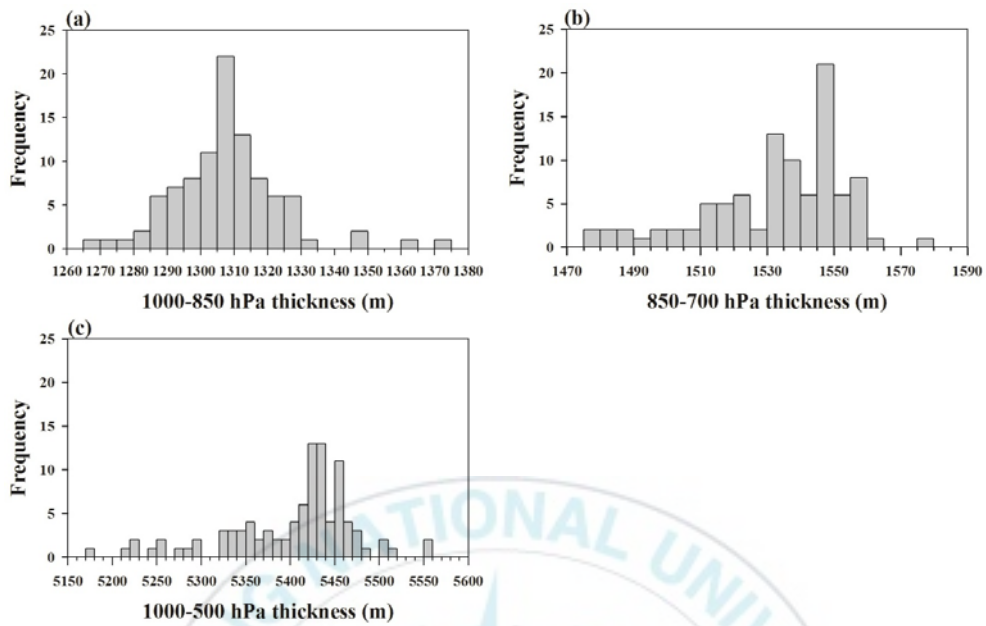


Fig. 9. The frequencies of the thickness values over a) 1000–850, b) 850–700, and c) 1000–500 thicknesses during freezing precipitation.

5.2. Use of the p-type nomogram

To predict precipitation patterns, the National Oceanic and Atmospheric Administration (NOAA) or the National Weather Service (NWS) in the United States uses the p-type nomogram, which has a range of 1260–1330 gpm with a 1000–850 thickness, and a range of 1500–1580 gpm for the 850–700 thickness, as seen in figure 10a. However A, and B in figure 10b are the areas that have been extended to present the thickness values used in this study. The gray pentagon area represents the area where freezing precipitation could occur in the USA, and it was defined as the freezing-precipitation occurrence area (FROA) (Fig. 10b). The FROA can be divided into three areas. The bottom part is the area where solid precipitation and freezing precipitation occur together, the middle part is the area where freezing precipitation mostly occurs but rain or snow could occur together, and the top part is the area where freezing precipitation and rain could occur together. If the thickness value approaches the FROA with the passage of time, this predicts the occurrence of freezing precipitation. However, in the case of Korea, only two cases were plotted in the FROA and this shows a significant difference from the USA. More severe problems are found in figure 10c. The empty gray circles denote the thickness data of 00, 06, 12, and 18 UTC from January 1 to February 28, 2014 in the substitution point (35.17°N, 126.89°E) of Gwangju, which has come from MERRA. Comparing the empty gray circles to the black circles, no distinct differences are found. Though the p-type nomogram has been

used for a long time in America, it is clear that its usefulness should be considered again if it is to be adopted in areas outside of the USA.

5.3. Freezing rain detector (FRAD)

Except for some cases explained in section 2-1, many cases of freezing precipitation are not recorded since they were not or could not be observed. For example, on January 20, 2014, seven accidents occurred on the Honam Expressway due to freezing precipitation, and 20 accidents occurred in the downtown area of Gwangju (Korean Broadcasting System [KBS], 2014). However, in the meteorological stations across the whole country, no occurrences of freezing precipitation were recorded. Another case is on January 28, 2014, when freezing precipitation occurred in Seoul (NewsY, 2014) without any reports of damage. The thicknesses of these two cases are shown in figure 10d, which are not included in the FROA.

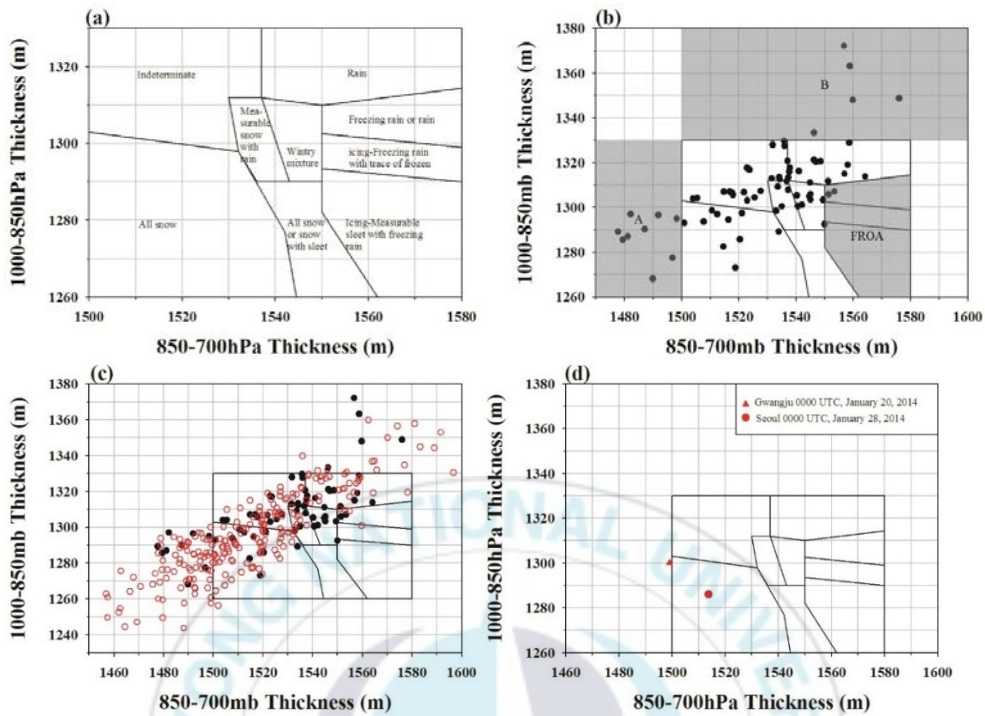


Fig. 10. a) P-type nomogram that the USA employs. b) Extended p-type nomogram used in this study. The FROA denotes the area where freezing rain is considered to be possible in the USA. A and B are areas of freezing precipitation that occurred in Korea, although it is the outward boundary of the USA p-type nomogram. Dots denote the occurrence of freezing precipitation. c) Same as in b), but for empty gray circles (data for 00, 06, 12, and 18 UTC from January 1 to February 28, 2014, Gwangju), d) two particular cases with extensive damage. The explanation is in the text

In these two cases, it is clear that meteorological stations could not observe all of the freezing precipitation, the reasons for which are as follows. Firstly, freezing precipitation is observed by the direct experience of an observer, rather than by automatic observation. Freezing precipitation that occurs outside the window for a moment and disappears at night is likely to be missed unless an observer stands outside and experiences it. In many cases, an observer would be unable to observe freezing precipitation while it freezes on the ground and melts away. However, even in this case, crops have already been damaged. This is because the growing points of plants (e.g., chili pepper, radish, and cabbage) have been frozen, and once they are frozen, they cannot recover, even after melting. Electric wires that are hung in the air could have already been broken due to freezing precipitation. If a traffic accident occurs, it could be disadvantageous in terms of insurance because there is no evidence that it has been due to freezing precipitation. Secondly, it normally occurs in mountainous areas and at night time with minimal human presence. Therefore, a device that can detect freezing precipitation automatically is required. Thus, an apparatus named the FRAD was proposed (Fig. 11). It has a number of branches, with a temperature sensor at the end of each branch from the conical support, and these form the main mechanism of the system. As soon as the falling liquid touches the temperature sensor, its temperature is observed and compared with one of the other sensors. Air temperature changes rapidly, but after freezing rain, the temperature of the frozen sensor shows a slow change and big differences from the other sensor. This can then be recognized as freezing rain.

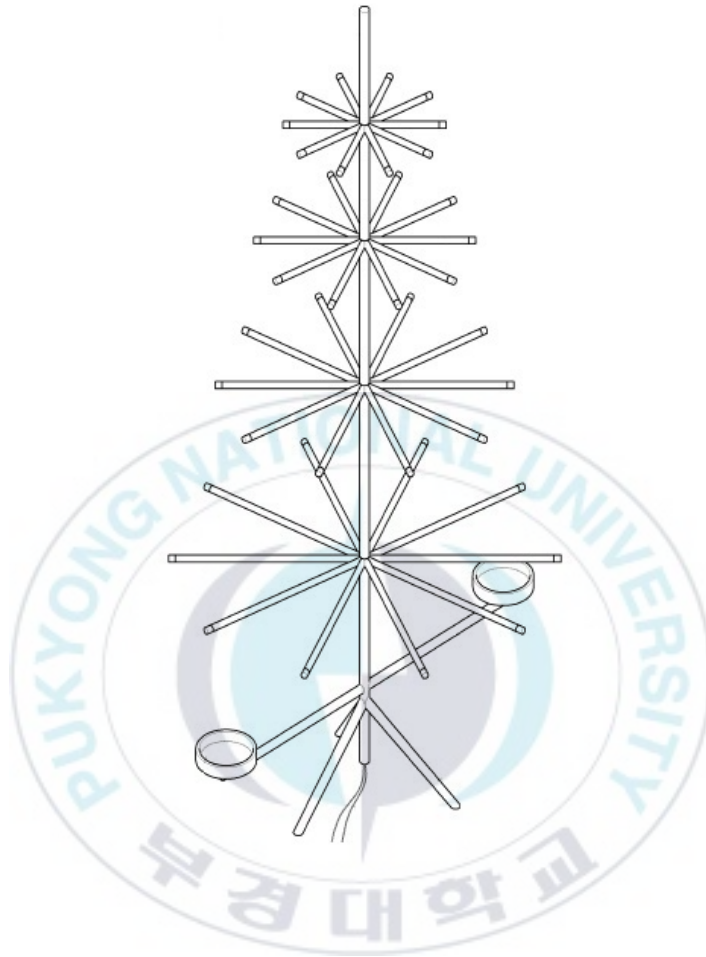


Fig. 11. A device on the apparatus for the automatic detection of freezing rain.

To enhance the effects, some ends are covered with fabric, or an ice-receiving plate is hung. It is desirable to install temperature sensors more densely than in the drawing shown in figure 11. When this device is used, every occurrence of freezing precipitation leaves a trace. Using this device, the traffic interruption in mountainous regions due to freezing precipitation and the resumption of traffic due to the melting of frozen roads can be checked without the need for a person to visit the places. However, the occurrence of freezing precipitation has strong local characteristics, and there could a difference between locations that are only several meters apart. Therefore, a much denser network of FRADs and a numerical model with ultra-fine grids are inevitable for the better prediction of freezing precipitation.

6. Summary and discussion

Freezing precipitation is a hazardous phenomenon that occurs not by itself, but in the process of the change from rain to solid precipitation or from solid precipitation to rain. Therefore, it has been very hard to predict for a long time. Regarding the change process, sometimes it occurs with or without damage. Though the possible area for the occurrence of freezing precipitation is very wide, it only occurs in small areas. Therefore, this study is a pioneering work in this area of research and should be viewed as a basic investigation. One hundred and two cases were collected through 123 weather stations (KMA: 77, North Korea: 27, and ROKAF:

19) from 2001 onward, and GST, SAT, vertical temperature profiles, thicknesses, and three kinds of synoptic weather charts, etc. have been investigated. They are summarized briefly in the abstract of this manuscript. The most important point relates to the problems that this study has found and that have to be solved to enable the successful prediction of freezing precipitation. Firstly, a better precipitation observation system is needed, not only for the detection of freezing precipitation, but also for other phenomena such as frost, hail, ice, etc., and although a piece of apparatus called the FRAD was proposed for this problem, it requires additional verification in the actual atmosphere. Secondly, many cases of freezing rain occur under conditions above freezing point. In five cases, both the GST and SAT levels were above 10 °C. This means that there are some processes that have yet to be recognized. Thirdly, it is a valuable finding that the FROA in Korea is entirely different from that of the USA, although the freezing process is the same throughout the world. P-type nomograms should be reproduced for the prediction of freezing precipitation in Korea. Fourthly, it has also been found that both a dense network of FRADs and a numerical model with ultra-fine grid points are required to solve this problem. It also clear that the more FRADs there are, the better the prediction will be of freezing-precipitation events.

Acknowledgement.

This work was funded by the Korea Meteorological Administration Research and Development Program under Grant CATER 2013-2020.

References

- Ashenden, R., and J. Marwitz, 1997: Turboprop aircraft performance response to various environmental conditions. *J. Aircraft*, **34**, 278-287.
- Atmospheric environment service, 1977: *Manual of surface weather observations*. 7th ed., Environment Canada, Atmospheric Environment Service, Toronto.
- Bennett, I., 1959: Glaze: Its meteorology and climatology, geographical distribution, and economic effects. Environmental Protection Research Division Tech. Rep EP-105, Headquarters, U.S. Army Quartermaster, Research and Engineering Command, Natick, MA, 217 pp. [NTIS AD-216668.]
- Brooks, C. F., 1920: The nature of sleet and how it is formed. *Mon. Wea. Rev.*, **48**, 69-73.
- Carrière, J. M., C. Lainard, C. Le. Bot, and F. Robert, 2000: A climatological study of surface freezing rain in Europe. *Meteor. Appl.*, **7**, 229-238.
- Changnon, S. A., 2003: Characteristics of ice storms in the United States. *J. Appl. Meteorol.*, **42**, 630-639.
- Cortinas, J. V. Jr., 2000: A climatology of freezing rain over the Great Lakes region of North America. *Mon. Wea. Rev.*, **128**, 3574-3588.
- Djuric, D., 1994: *Weather analysis*. Prentice hall, 304 pp.
- Donaldson, N. R., and R. E. Stewart, 1989: On the precipitation regions within two

- storms affecting Atlantic Canada. *Atmos.-Ocean*, **27**, 108-129.
- Gay, D. A., and R. E. Davis, 1993: Freezing rain and sleet climatology of the southeastern USA. *Climate Res.*, **3**, 209-220.
- Heppner, P. O., 1992: Snow versus rain: looking beyond the "magic" numbers. *Wea. Forecasting*, **7**, 683-691.
- Hong, S.G., 2013: *Analysis of weather and weather forecasts*. Gyohakyungusa, 575 pp. (In Korean)
- Houston, T. G., and S. A. Changnon, 2007: Freezing rain events: a major weather hazard in the conterminous us. *Nat. Hazards*, **40**, 485-494.
- Huffman, G. J., and G. A. Norman Jr., 1988: The super cooled warm rain process and the specification of freezing precipitation. *Mon. Wea. Rev.*, **116**, 2172-2182.
- KBS, 2014: Surprise of freezing rain with traffic accident at Jan 28, 2014. (In Korean)
- http://news.kbs.co.kr/news/NewsView.do?SEARCH_NEWS_CODE=2793293&ref=A
- Keeter, K. K., and J. W. Cline, 1991: The objective use of observed and forecast thickness values to predict precipitation type in North Carolina. *Wea. Forecasting*, **6**, 456-469.
- _____, K. K., S. Businger, L. G. Lee, and J. S. Waldstreicher, 1995: Winter Weather Forecasting throughout the Eastern United States. Part III: The

- Effects of Topography and the Variability of Winter Weather in the Carolinas and Virginia. *Wea. Forecasting*, **10**, 42-60.
- Keyser, D., M. J. Reeder, and R. J. Reed, 1988: A generalization of Petterssen's frontogenesis function and its relation to the forcing of vertical motion. *Mon. Wea. Rev.*, **116**, 762-781.
- Kim, J. H., K. R. Kim, K. Y. Nam, M. K. Seok, and S. J. Lee, 2009: The case analysis of freezing rain. *Extended Abstracts, Proceedings of the spring meeting of the Korean Meteorological Society*, 250-251. (In Korean)
- KMA, 2002: *Manuals for ground weather observation*. Korea Meteorological Administration, 243 pp. (In Korean)
- Kong, Y. S., Y. D. Kim, and Y. W. Chae, 2012: Correlation Analysis between freezing rain and application amount snow removal. Korea Expressway Corporation Report, 49 pp. (In Korean)
- Koolwine, T. 1975: Freezing rain. MS. Thesis, University of Toronto, 92 pp.
- Korean Meteorological Society and KMA, 2013: *Atmospheric sciences terminology*. 1042 pp. (In Korean)
- Martner, B. E., J. B. Snider, R. J. Zamora, G. P. Byrd, T. A. Niziol, and P. I. Joe, 1993: A remote-sensing view of a freezing rain storm. *Mon. Wea. Rev.*, **121**, 2562-2577.
- Mckay, G. A., and H. A. Thompson, 1969: Estimating the hazard of ice accretion in

- Canada from climatological data. *J. Appl. Meteorol.*, **8**, 927-935.
- Meisinger, C. L., 1920: The precipitation of sleet and the formation of glaze in the eastern United States, January 20 to 25, 1920, with remarks on forecasting. *Mon. Wea. Rev.*, **48**, 73-80.
- Mireles, M., K. L. Pederson, and C. H. Elford, 2003: Meteorological Techniques (Revision 21 Feb 2007). Air Force Weather Agency Tech. Note 98-002, Offutt AFB NE 68113, 237 pp.
- NewsY, 2014: "slip" cause by "freezing rain," caution icy roads during Lunar new year's day. (in Korea)
[http://news.naver.com/main/read.nhn?mode=LSD&mid=sec&sid1=102&oid=422 &aid=0000046861](http://news.naver.com/main/read.nhn?mode=LSD&mid=sec&sid1=102&oid=422&aid=0000046861) at 28 Jan, 2014.
- Ohtake, T., 1963: Hemispheric investigation of warm rain by radio sonde data. *J. Appl. Meteorol.*, **2**, 594–607.
- Park, C. G., and H. R. Byun, 2014: 3 cases of multiple occurrences of freezing rains in a day over Korean Peninsula, (20060112, 20080111, 20090222). In review at Asia-pacific journal of atmospheric Sciences.
- Petterssen, S., 1936: Contribution to the theory of frontogenesis. *Geofys. Publ.*, **11**, 1-27.
- Pike, W. S., 1995: Extreme warm frontal icing on 25 February 1994 causes an aircraft accident near Uttoxeter. *Meteor. Appl.*, **2**, 273-279.
- Rauber, R. M., L. S. Olthoff, M. K. Ramamurthy, and K. E. Kunkel, 2000: The

- relative importance of warm rain and melting processes in freezing precipitation events. *J. Appl. Meteorol.*, **39**, 1185-1195.
- _____, R. M., L. S. _____, M. K. _____, D. Miller, and K. E. _____, 2001: A Synoptic Weather Pattern and Sounding-Based Climatology of Freezing Precipitation in the United States East of the Rocky Mountains. *J. Appl. Meteorol.*, **40**, 1724-1747.
- Sand, W., W. Cooper, M. Politovich, and D. Veal, 1984: Icing conditions encountered by a research aircraft. *J. Appl. Meteorol.*, **23**, 1427-1440.
- Stallabrass, J. R., 1983: Aspects of and testing. *Proc. First Intl. Wkshp. Atmos. Icing of Structure*, Hanovar, NH, CRREL, 67-74.
- Stewart, R. E., 1985: Precipitation types in winter storms. *Pure Appl. Geophys.*, **123**, 597-609.
- Steenburgh, W. J., C. F. Mass, and S. A. Ferguson, 1997: The influence of terrain-induced circulations on wintertime temperature and snow level in the Washington Cascades. *Wea. Forecasting*, **12**, 208-227.
- Stuart, R. A., and G. A. Isaac, 1999: Freezing precipitation in Canada. *Atmos.-Ocean*, **37**, 87-102.
- Sun, J., and S. Zhao, 2010: The impacts of multi scale weather systems on freezing rain and snowstorms over southern China. *Wea. Forecasting*, **25**, 388-407.
- Weber, E. M., 1998: Freezing Precipitation. Air Force Weather Agency Tech. Note 98-001, Offutt AFB NE 68113, 132 pp.
- WMO, 1995: World Meteorological Organization's Manual on Codes. WMO-No.

306, Geneva. 503 pp.

Young, W. H., 1978: Freezing precipitation in the southeastern United States. M. Sc. thesis, Texas A&M University, 123 pp.

Zhou, W., J. C. L. Chan, W. Chen, J. Ling, J. G. Pinto, and Y. Shao, 2009: Synoptic-scale controls of persistent low temperature and icy weather over southern China in January 2008. *Mon. Wea. Rev.*, **137**, 3978-3991.



Acknowledgement (Korean)

감사의 글

감사의글을 적고 있는 지금 이 순간이 되어서야 석사학위를 무사히 마무리 하였다는 것이 실감이 납니다. 지난 시간들을 돌아보니 정말 많은 일들을 겪었고, 많은것을 배우고 알아갔었습니다. 또한 석사과정 동안의 좋은 분들을 만나 큰 힘이 되었습니다. 또한, 부족한 석사논문에 성심 성의껏 심사해주시고 논문의 완성도를 높일수 있게 날카로운 조언을 아끼지 않으신 김재진 교수님과 권병혁 교수님에게 큰 감사를 드립니다. 또한, 제자들에게 사랑하는 마음과 지식을 나눠주셨던 정형빈 교수님, 이동인 교수님, 오재호 교수님, 옥곤 교수님에게 감사드립니다.

지도 교수님이신 변희룡 교수님에게 정말 감사합니다. 군복무 후 복학을 한 제가 진로와 삶의 방향에 주저하며 갈팡질팡할때에 교수님의 수업을 들으면서 주저하지말고 목표를 향해 나아갈수 있는 원동력이 되었주셨습니다. 그로인해 연구실 입학에 희망하였으며, 입학 조건을 만족하기위해 1년동안 제가 학업에 열중하며 학업속에서 재미를 느낀것에대해 너무나도 큰 기뻐고, 그러한 힘이 석사과정 마무리에 도움이 되었습니다. 특히 인생의 가치를 학문에서 찾으시는 교수님에게서 앞으로의 학문의 길에서도 교수님의 말씀과 가르침을 잊지 않도록 하겠습니다.

다음으로 먼 타지에서 학업의 길을 가는 아들이자 남동생의 뒷바라지 해주느라 고생하신 아버지, 어머니, 누나에게 존경과 감사를 드립니다. 명절에 한번 얼굴을 맞대어 이야기 할 수밖에 없었지만, 그때마다 아버지 어머니의 한마디 한마디가 제가 가고 있는 학문의 길에 포기 하지않고 끝까지 이뤘 갈수 있는 큰 힘이 되었습니다. 특히, 누나에게는 개인적으로 미안하고 고맙습니다. 가난한 집안이었기에 먼저 사회에서 일하는 누나에게 학업을 선택하여 생겼던 모든 일들에대해 미안합니다. 그럼에도 불구하고 동생이 타지에서 혹여 굶고 지낼까봐 여분의 돈을 쥐어준 누나가 정말 고맙고 소중합니다.

여기에 오기까지에는 MDR연구실의 구성원들도 큰 도움이 되었습니다. 처음 들어간 연구실에서 따듯하게 맞아주신 선배님들도 있었고 연구실이 또하나의

집처럼 안정감있었지만, 다들 졸업하고 가버린 뒤에는 아쉬웠습니다. 차분하고, 항상 주어진일에 결단력있었던 진아 누나는 첫 포스터 발표에 큰 도움을 주었고 많은 도움을 주신점에 고마웠습니다. 교수님께서 가끔 이름을 헛갈려 했던 보라누나와 소라누나는 정말 똑똑한 선배들이었고 학문에있어서 필요한 프로그래밍에 매우 큰 도움을 주신 고마운 선배들이었습니다. 창균형님은 연구실에서 남자가 저와 형님뿐이었기에 공감대가 많아 이야기를 많이 나누었으며, 주어진일을 미루지 않고 묵묵히 하던 모습이 기억에 남습니다. 동기였던 수정이는 똑부러지게 일하는 모습이 가장 인상이 남습니다. 동기인 가빈이는 저보다 조금더 일찍 연구실에 들어와 킷킷히 공부하던 모습과 한가지 일에 집중하면 좋은 결과를 보여주는 좋은 동기였습니다. 그리고 항상 옆자리에 앉았던 후배 유진이는 항상 제가 장난을 쳤지만 잘받아줘서 고마웠고 덕분에 연구실이 더 즐거웠던거 같습니다. 후배 지인이라도 즐거운 연구실생활에 큰 도움이 되었습니다. 후배 희내는 같은 졸업동기이며 같은 안동권가의 자손입니다. 졸업후 박사진로를 희망하는 동생이기에 정말 잘되었으면 좋겠습니다. 마지막으로 아직 학부생인 용덕이에게는 앞으로의 길이 정말 잘되길 진심으로 기원합니다.

그리고 중학교때부터 친구였던 태우, 정욱, 재환, 병관이는 제가 학과생활이 힘든시기마다 힘이되어준 고마운 친구들입니다. 특히 태우와 재환이도 다른 학업에서 석사과정을 하고 있는데, 이를 잘 이겨내고 잘해내리라 믿습니다.

대학교에와서 가장 많은 추억 만들어주었고 많은 도움이 되었던 동기들 모임인 ing캠의 상아, 정현, 정은, 효준, 원호, 종현이에게 정말 고맙습니다. 이들중 같은 석사 졸업 동기인 효준이와 종현이는 석사 졸업기간 동안 서로 많은 도움이 된 친구들입니다. 아직 석사과정인 원호는 석사졸업을 잘 끝마칠수 있을것이라 믿습니다. 정현이는 하고 있는 공부의 결과가 잘 나오길 바랍니다. 학부 1학년에 친해졌던 태운이, 민식이는 석사과정을 가는 저와 많은 이야기들과 정보를 제공해준 좋은 친구들입니다. 친구들 각자의 길에 있어서 잘되길 바랍니다. 이외에도 도움을 준 친구들, 선배, 후배님들 등등 다른분들을 일일이 열거하지 못해 죄송할 따름이며 감사합니다.